PREDICTIVE MODELLING FOR PHOTOVOLTAIC SOLAR POWER GENERATION WITH COMPARATIVE ANALYSIS BETWEEN DEEP LEARNING AND STATISTICAL TIME SERIES MODELS.

ABSTRACT

This study presents a comprehensive comparative analysis between deep learning and statistical time series models for predicting photovoltaic (PV) solar power generation. By incorporating convolution, which can learn complexity from raw data, and meteorological features strongly correlated with PV solar power generation, the deep learning models demonstrated improved performance in prediction, surpassing conventional statistical methods. Among these methods, the Convolutional Neural Network with Gated Recurrent Unit (CNN-GRU) multivariate model emerged as the best overall, achieving Mean Absolute Error (MAE), Mean Squared Error (MSE), Root Mean Squared Error (RMSE), and Correlation Coefficient (R) values of 0.235, 0.089, 0.298, and 0.973, respectively. This performance outperformed related studies in forecasting the electricity generated from PV solar panels across multiple time steps. The computational time for prediction in statistical models was significantly faster than in deep learning models, making them a better fit for rapid short-term forecasts. Conversely, deep learning models are more suitable for long-term predictions, where computational speed is of lesser importance. This research significantly contributes to advancing sustainable energy solutions and strategies for mitigating climate change.

1.0 INTRODUCTION

The importance of sustainable energy is essential to our world today, given its impact in addressing the urgent issue of climate change. Since the Covid-19 pandemic, demands for sustainable and clean energy sources of electricity have grown significantly, while conventional forms of energy have been on the decline (IEA, 2020). PV solar system is one of the most common types of sustainable energy solutions, involving the transformation of abundant and renewable sunlight into electricity. Electricity derived from PV solar systems entirely depends on meteorological elements such as solar radiation, relative humidity, and temperature (Das et al., 2018). For proper optimization of the PV solar system generated power, accurate prediction of this output power over time is required to aid in cost reduction, thereby increasing accessibility (Jones, 2014). Improved accuracy in forecasting PV power output enhances system reliability and enables the implementation of efficient load management strategies (Huang et al., 2015).

The objective of this study is to assess and compare the predictive performance of various variants of Recurrent Neural Networks (RNN) such as the Long Short-Term Memory (LSTM), Bidirectional Long Short-Term Memory (Bi-LSTM), and Gated Recurrent Unit (GRU), against Autoregressive Moving Average (ARMA) and Autoregressive Integrated Moving Average (ARIMA) time series models in forecasting PV solar power generation. To facilitate a thorough analysis, Convolutional Neural Networks (CNN) and meteorological data will later be integrated into the deep learning models, while seasonality will be incorporated into the statistical models.

2.0 BACKGROUND

Wang et al. (2019) proposed a novel deep learning approach called the “Multiple CNN” which was designed to solve the problem of periodic multivariate time series prediction for long-term cycle, closeness and short-term cycle with the implementation of CNN. This approach by Wang et al. (2019) gives a more accurate prediction for all forms of periodic data with a better performance when compared to traditional time series model such as the ARMA and ARIMA models. According to Wang et al. (2019), stacking multiple CNN is more suitable for learning sequence and has less computational requirement when compared to the RNN, LSTM and GRU models. Residual network was used to deepen the CNN network layers to help capture sequencing according to the authors. Two data set were used in this literature, the weather in traffic dataset and solar power generation data set which were a 48-month hourly data gotten from the California department of transportation and a single year 10-minute time step sample data from 137MW PV power plant in Alabama, respectively. For this research, we are more concerned with the result performance of the latter for better analysis, where predictions were made for the next 24-timestep horizon, with each step covering a span of 10 minutes. The “Multiple CNN” model performed best when compared to other models, having an RMSE, RMAE, and R of 0.461, 0.262 and 0.897, respectively for the 24-timestep horizon evaluation.

Sharadga et al. (2019) elaborated on the importance of accuracy in predicting power generation in a PV solar system. Sharadga et al. (2019) was able to compare several statistical and artificial intelligence (AI) models in search for better a prediction. In this literature, Sharadga et al. (2019) proposed the BI-LSTM algorithm which showed to have the most accurate prediction for a single timestep horizon when compared to other models such as the Layer Recurrent Neural Network (LRNN), LSTM, ARIMA, ARMA and others in forecasting PV solar power generation, although these results tend to change as the predicted time stamp increases. Unlike the literature by Wang et al. (2019), Sharadga et al. (2019) made use of an hourly time step dataset from a 20MW grid-connected PV station in China and were only able to forecast with a timestep horizon of 3 hours, where the LRNN outperformed with an RMSE of 1.805 and an R value of 0.895.

Bamisile et al. (2020) made use of Artificial Neural Network (ANN) models of different architecture for predicting solar irradiance and PV power generation in Nigeria. The dataset used in this literature was gotten from six different states in Nigeria, each having hourly time steps. Bamisile et al. (2020) were able to compare the performance of each dataset using different models, adding meteorological data along with the years, months, days and hours as feature values in search for better accuracy. The best performing ANN model in this literature for predicting PV power generation achieved an RMSE, MAE and R value of 42.447, 10.418, and 0.877 respectively.

From the literature reviews, we can observe that there is a growing interest in using deep learning methods for time series prediction of solar power generation due to its more profound accuracy when compared to traditional statistical models. The key steps undertaken for this research can be summarized as follows:

- The PV solar power and meteorological dataset from the year 2006, collected at the same time and location will be used to generate the PV solar power data for 2007 to 2021. This will be achieved with the help of a Support Vector Regression (SVR) model.
- An average monthly power generation dataset is utilized for long-term prediction, with the objective of forecasting a time horizon for the next 24 months using both deep learning and statistical methods, as mentioned earlier.
- Performance enhancement through the inclusion of convolutional layers and the utilization of multivariate data from meteorological datasets for deep learning modelling, alongside the incorporation of seasonality within the statistical model

3.0 METHODOLOGY

In this section, we will be focusing on the process workflow and methods used for this project. Figure 1 shows the breakdown structure from data collection all the way to predictions.

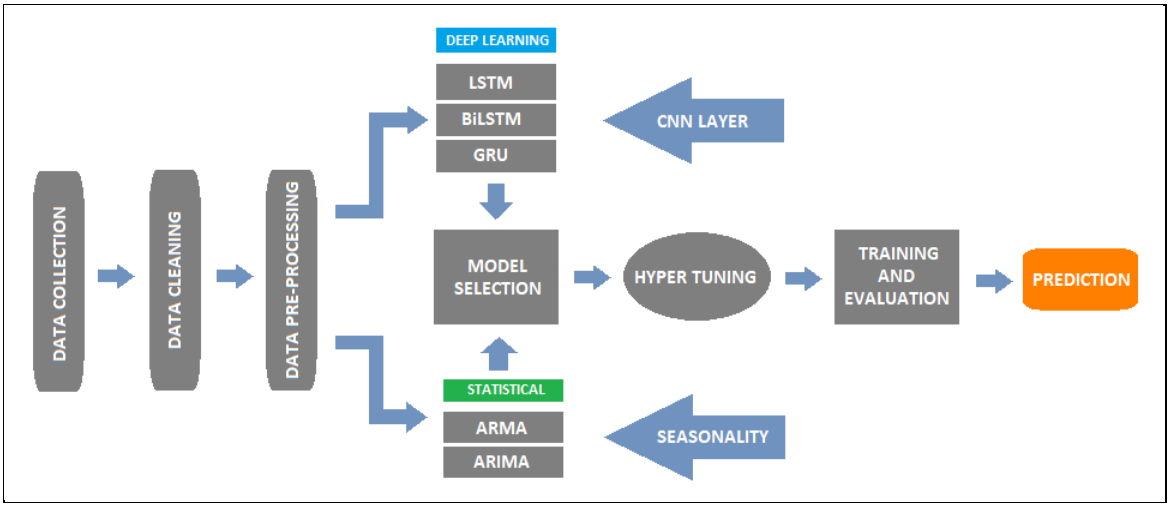

Figure 1. *Process Flow Diagram of the methods.*

3.1 Data Collection and Preparation

For this project, we utilized two distinct datasets:

1. A time series univariate dataset comprising 35MW photovoltaic (PV) solar power generation data for the year 2006, was obtained from the National Renewable Energy Laboratory (NREL, 2019).
2. A multivariate meteorological dataset with 46 columns spanning from the year 2006 to 2021, sourced from the National Solar Radiation Database (NSRDB, 2019).

Both datasets were collected at regular 60-minute intervals and originated from a specific location in Texas, United States, with identical longitude and latitude coordinates of 32.4 and -94.7, respectively Data cleaning was performed on the meteorological data, which involved the removal of null values and irrelevant columns. Additionally, new column names were established, incorporating the International System (SI) unit for some of the existing columns.

Since we know that PV solar power generation entirely depends on meteorological elements as earlier stated, the power generation data for the year 2007 to 2021 was derived using model-based feature creation with the help of SVR.

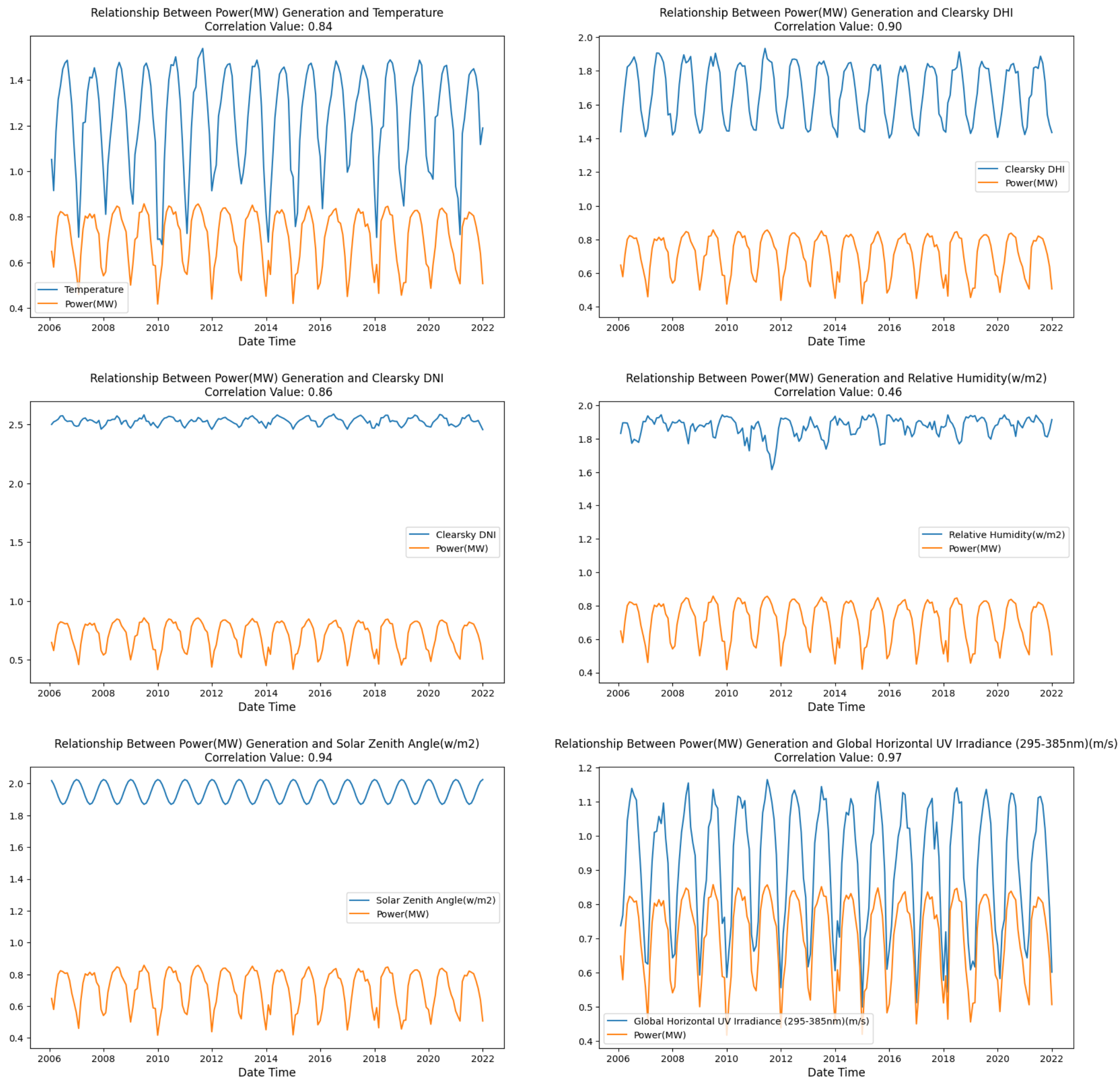

Figure 2. *Relationship between power generation and selected feature variables.*

This feature engineering technique made use of the 2006 power generation data as the target variable, consisting of 8760 rows, while six (6) selected features from the meteorological data were used as the independent variables, which includes Temperature, Clearsky Diffuse Horizontal Irradiance (DHI), Clearsky Direct Normal Irradiance (DNI), Relative Humidity, Solar

Zenith Angle, and Global Horizontal UV Irradiance. These features were obtained after applying forward feature selection. The SVR is a linear regression model used to predict the target variable (y) based on the independent variables ($\vec{x}$).

$$y = \vec{w} \cdot \vec{x} + b \tag{1}$$

The goal of this model is to find the optimal values for the weight vector ($\vec{w}$) and the bias (b) to best minimize the value between the predicted and the actual target. Grid-Search parameter tuning was later applied to enhance our model accuracy, resulting to an R^2 percentage value of 92.4%. The total time series data was then converted from hourly to monthly timestamp of 192 rows using mean average. Figure 2 shows the relationship between power generation and selected feature variables from our monthly time series data.

3.2 Deep Learning Forecasting Model

For the deep learning model, the data was split into training, validation, and testing sets with a ratio of 6:1:1, respectively. The testing set consisted of data from the years 2020 and 2021, as shown in Figure 3.

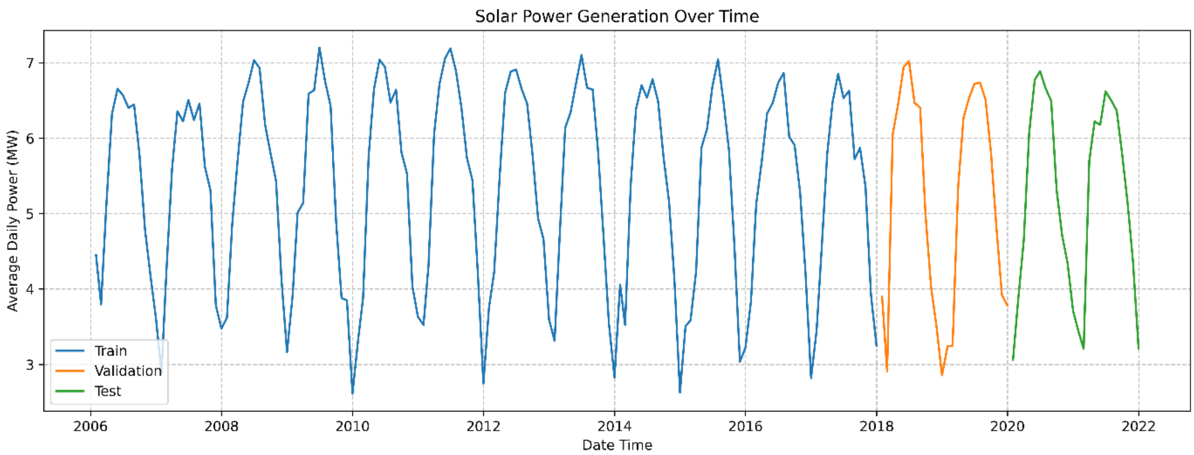

Figure 3. *Data splitting of the deep learning model.*

3.2.1 Windowing

Windowing is a machine learning technique that involves dividing our time series data into smaller, fixed-size segments or windows, each consisting of consecutive data points (Moroney, 2019). This allows us to sequentially move through the data with a given time step, creating input features and corresponding labels for training predictive models for our deep learning neural network.

Input Features = $[X_1, X_2, \ldots, X_{12}], [X_2, X_3, \ldots, X_{13}], \ldots, [X_3, X_4, \ldots, X_{191}]$

Labels = $[X_{13}], [X_{14}], \ldots, [X_{192}]$ (2)

From equation 2, a window size of 12 was used for the input features while the corresponding label is the next time stamp after each window. This technic is also applicable to multivariate time series which have multiple features where the width of the corresponding labels matches the number of features.

3.2.2 Recurrent Neural Network (RNN)

Artificial neural networks such as the RNN are designed to process sequential data which has been established using windowing. Although there are a few drawbacks to the simple RNN architecture such as difficulty in accessing long term historical information resulting in vanishing gradient, and its inability to consider future input for current modelling (Amidi & Amidi, 2021). These issues can be addressed using RNN variants such as LSTM, Bi-LSTM, and GRU.

According to Brownlee (2018), the LSTM can capture long-term connections and memory, although the GRU is like the LSTM but has a lesser complexity. For the case of utilizing future input information to enhance prediction, a Bidirectional RNN model such as Bi-LSTM utilizes two LSTM architectures in a single time step ($x^{<t>}$).

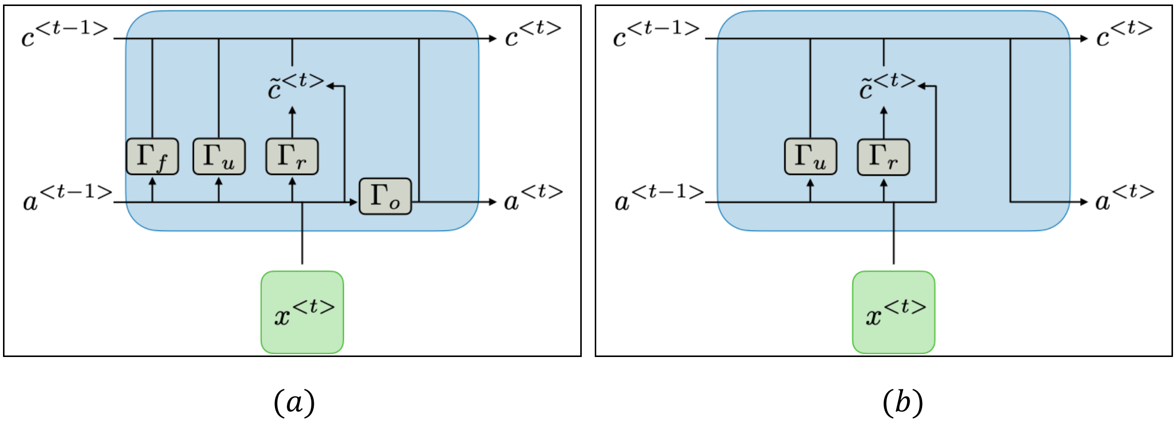

Figure 4. *The architecture of* (a) *LSTM cell and* (b) *GRU cell (Amidi & Amidi, 2021).*

Four gates were used in the LSTM architecture, the update gate (Γ_u), the relevance gate (Γ_r), the forgot gate (Γ_f), and the output gate (Γ_o) unlike the GRU which has only two as shown in Figure 4. The forgot gate and the relevance gate both have similar characteristics and are sometimes categorized as one. For both the LSTM and the GRU, the cell input state ($\tilde{c}^{<t>}$), output state ($c^{<t>}$), and previous state ($c^{<t-1>}$) will be implemented during the training process.

The gates Γ are defined by this equation (Amidi & Amidi, 2021):

$$\Gamma = \sigma(Wx^{<t>} + Ua^{<t-1>} + b) \tag{3}$$

where W, U, *and* b are parameters to the gate while, $a^{<t-1>}$ and σ are the hidden state from previous step and the sigmoid activation function respectively.

The equation for the cell input state is defined as follows (Amidi & Amidi, 2021):

$$\tilde{c}^{<t>} = \tanh(W_c[\Gamma_r \star a^{<t-1>}, x^{<t>}] + b_c) \tag{4}$$

where the $\star$ sign denotes vector multiplication and tanh is the activation function.

The equation for both sigmoid (σ) and hyperbolic tangent(tanh) activation function is as shown.

Sigmoid (σ):

$$g(z) = \frac{1}{1 + e^{-z}} \tag{5}$$

Hyperbolic tangent(tanh):

$$g(z) = \frac{e^{z} - e^{-z}}{e^{z} + e^{-z}} \tag{6}$$

In addition to the parameters, a return sequence will be used for each of the selected RNN models to ensure the entire output sequence from the previous layer is passed to the next RNN layer.

3.2.3 Convolution Layer Implementation

The convolutional layers can be used to extract features from the time series data at the initial stage of the architecture (Pan & Zhou, 2020). During the cause of this project, a single dimensional convolutional input layer followed by a MaxPooling layer was added to each of the RNN architectures, resulting in a CNN-RNN hybrid model. This combination allows the model to learn both spatial and temporal features from the data, potentially leading to improved performance.

Parameter compatibility is an aspect to consider for such hybrid model to be able to know the appropriate output size for the CNN layer. The output (O) size after applying convolution is influenced by the input dimension (W), filter size (K), stride (S), and padding (P).

The equation to calculate the expected output dimension as shown (Ng et al., 2017):

$$O = \frac{\mathrm{W} - \mathrm{K} + 2\mathrm{P}}{\mathrm{S}} + 1 \tag{7}$$

The RELU is used as the activation function for the CNN layer as shown (Ng et al., 2017):

$$g(z) = max(0, z) \tag{8}$$

For the time series models, the application of both univariate and multivariate approaches included a one-dimensional CNN layer and a pooling layer, as shown in Table 1.

Table 1. *Deep Learning Model Layers.*

RNN Models (Univariant)			CNN-RNN (Univariate)			CNN-RNN (Multivariant)		
LSTM	Bi-LSTM	GRU	Conv1D	Conv1D	Conv1D	Conv1D	Conv1D	Conv1D
LSTM	Bi-LSTM	GRU	MaxPool	MaxPool	MaxPool	MaxPool	MaxPool	MaxPool
Dense	Dense	Dense	LSTM	Bi-LSTM	GRU	LSTM	Bi-LSTM	GRU
Dense	Dense	Dense	LSTM	Bi-LSTM	GRU	LSTM	Bi-LSTM	GRU
-	-	-	Dense	Dense	Dense	Dense	Dense	Dense
-	-	-	Dense	Dense	Dense	Dense	Dense	Dense

3.3 Statistical Forecasting Model

Both ARIMA and ARMA are conventional statistical model that combines Autoregression (AR), and Moving Average (MA) techniques (Brownlee, 2018).

AR is a regression model that depends on past values to make predictions, while the MA model uses analysis of the errors from past predictions to improve on the current time period (Rajbhoj, 2019).

The (I) in ARIMA stands for Integrated. This means that instead of predicting the actual values of a time series at each time step, it will focus on predicting the changes in the time series (Shweta, 2021). It represents the number of times the data needs to remove the trend component to make the data stationary.

The AR, I and MA are represented with the parameters (p, d, q) respectively. An ARIMA model can be obtained when the parameters are greater than 0. When d = 0, you have the ARMA model.

The statistical models can be defined by the equation (Hariharan, 2020):

$$\hat{y}_t = \mu + \varphi_1 y_{t-1} + \ldots + \varphi_p y_{t-p} - \theta_1 e_{t-1} - \ldots - \theta_q e_{t-q} \tag{9}$$

where μ is a constant value, while $\varphi_1 y_{t-1} + \ldots + \varphi_p y_{t-p}$ and $\theta_1 e_{t-1} - \ldots - \theta_q e_{t-q}$ represents the AR lagged value of y and MA lagged error respectively.

To assess stationarity, analytical and visualization techniques employed the Dickey-Fuller test and Rolling Statistical methods. The former includes test statistics, p-value, and critical values, where a p-value exceeding 0.05 signifies the necessity to reject the null hypothesis of non-stationarity.

Implementing seasonality to these models could aid in its prediction since we are working with a seasonal data. Unlike the ARMA and ARIMA models, we will be considering some additional parameters such as the Seasonal Autoregression (SAR), Seasonal Integrated order (SI), Seasonal Moving Average (SMA) and the Seasonal periodicity, which can also be referred to as parameters (P, D, Q, s). The SARIMA total parameters which combine seasonality to the statistical models can be represented as $(p, d, q) \times (P, D, Q, s)$.

3.4 Performance Enhancement Techniques

To optimize on the performance for the deep learning model, experimentation was conducted with various batch sizes, along with the implementation of a Learning Rate Scheduler (LRS) to determine the appropriate learning rate value for each model.

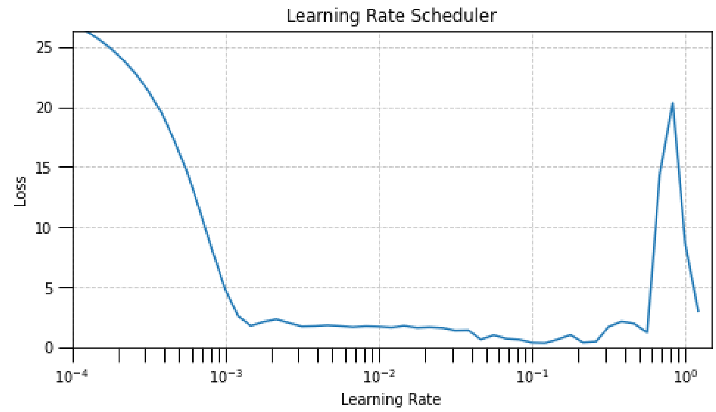

Figure 5. *Graphical Representation using the LRS for the LSTM deep learning model.*

The best learning rate will be slightly before the steepest descent point which is about 10^{-3} from the representation shown in Figure 5.

Partial Autocorrelation (PACF) and Autocorrelation (ACF) functions are visual methods to determine the parameters for the statistical models based on significant lags as shown in Figure 6. These methods can be re-evaluated using the Akaike Information Criterion (AIC) and Bayesian Information Criterion (BIC) numbers to achieve the values for p and q.

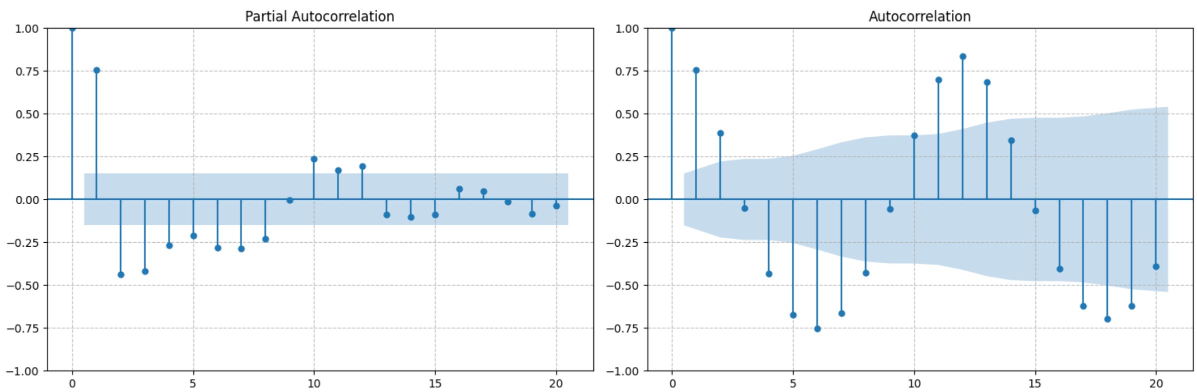

(a)

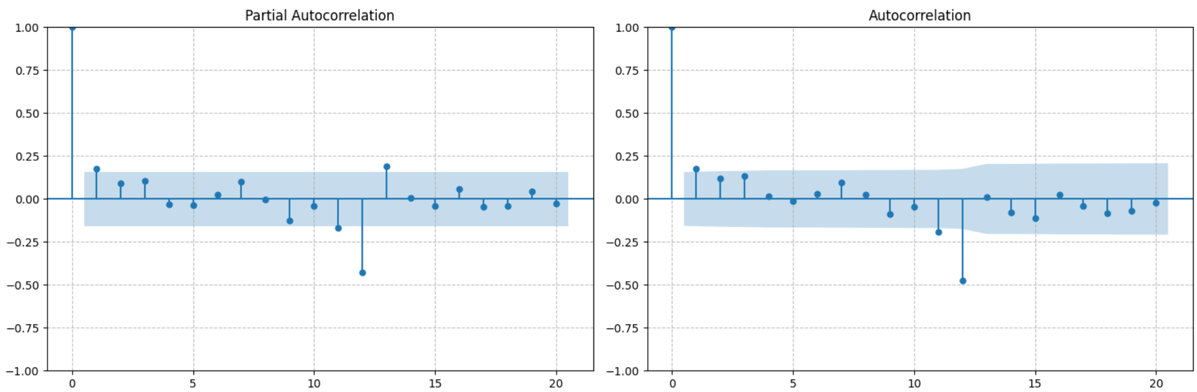

(b)

Figure 6. *PACF and ACF: (a) log power output, and (b) seasonal differenced log power output.*

4.0 RESULT

For this study, four evaluation metrics were used to ascertain the prediction accuracy for both deep learning and statistical model. The MAE, MSE, and RMSE measures the error between the actual values and the predicted values for each of the models, whereas R quantifies the strength and direction of the linear relationship. The best model is expected to have the lowest error and the highest correlation coefficient.

Table 2. *Evaluation results for the deep learning models.*

	LSTM	BiLSTM	GRU	CNN-LSTM	CNN-BiLSTM	CNN-GRU	CNN-LSTM (m)	CNN-BiLSTM (m)	CNN-GRU (m)
MAE	0.285	0.263	0.292	0.248	0.271	0.264	0.272	0.255	0.235
MSE	0.135	0.139	0.163	0.103	0.124	0.118	0.113	0.109	0.089
RMSE	0.367	0.373	0.404	0.321	0.352	0.344	0.336	0.330	0.298
R	0.959	0.964	0.953	0.968	0.965	0.967	0.971	0.966	0.973
CT (ms)	23.59	39.51	20.11	22.90	40.19	21.19	23.62	42.34	21.30

From Tables 2 and 3, it is evident that the CNN-GRU multivariate (m) deep learning model and the SARIMA with zero seasonal differencing (D) exhibit the most favourable performance based on their evaluation. The CNN-GRU (m) model achieves MAE, MSE, RMSE, and R values of 0.235, 0.089, 0.298, and 0.973 respectively, while the SARMA model gives corresponding values of 0.293, 0.134, 0.366, and 0.964.

Table 3. *Evaluation results for the statistical models.*

	ARMA d=0	ARIMA d=1	SARIMA D=1	SARMA D=0
MAE	0.410	0.406	0.317	0.293
MSE	0.231	0.227	0.166	0.134
RMSE	0.481	0.476	0.407	0.366
R	0.936	0.938	0.953	0.964
CT (ms)	0.96	0.72	0.70	0.88

The computational time of prediction (CT) was also included in our evaluation for both district models. For the deep learning model GRU model had the lowest CT at 20.11 (ms) while the statistical SARIMA model had a value of 0.70 also shown in Tables 2 and 3 respectively.

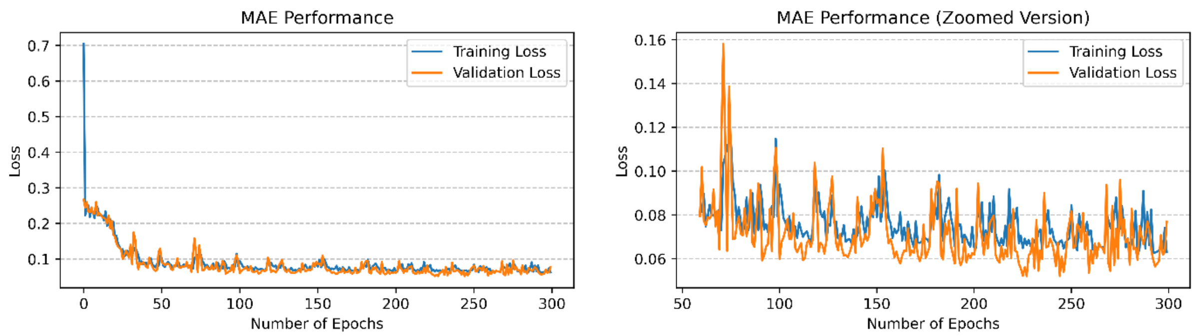

Figure 7. *Training and validation loss for the CNN-GRU (m) model.*

Comparing the training and validation loss of the CNN-GRU (m) deep learning model is essential to assess both its performance and generalization, as illustrated in Figure 7. The training loss and validation loss both appear to decrease over the course of the training epochs. This is a positive sign, indicating that the model is learning from the training data and generalizing its knowledge to the validation data.

Logarithmic transformations were applied to the multivariate deep learning and statistical data to enhance scaling and stationarity, respectively. Subsequently, after making predictions, these transformations were reversed using the exponential function for the purpose of evaluation.

Table 4. *Top 5 AIC and BIC values for the SARMA (D=0) model parameters.*

(p, d, q)	AIC	BIC	(P, D, Q, s)	AIC	BIC
(2, 0, 3)	**-239.44**	**-217.57**	**(3, 0, 1, 12)**	**-275.07**	**-240.71**
(3, 0, 4)	-232.15	-204.04	(4, 0, 2, 12)	-274.98	-234.37
(2, 0, 5)	-230.46	-202.34	**(1, 0, 1, 12)**	**-274.47**	**-246.35**
(4, 0, 5)	-229.39	-195.03	(2, 0, 3, 12)	-272.76	-235.27
(2, 0, 2)	-228.35	-209.61	(2, 0, 2, 12)	-272.58	-238.22

Since it takes much lesser computational time for prediction using the statistical method, a function was created to iterate through different parameters of the statistical model to ascertain the best parameter combination with the lowest AIC and BIC as shown in Table 4.

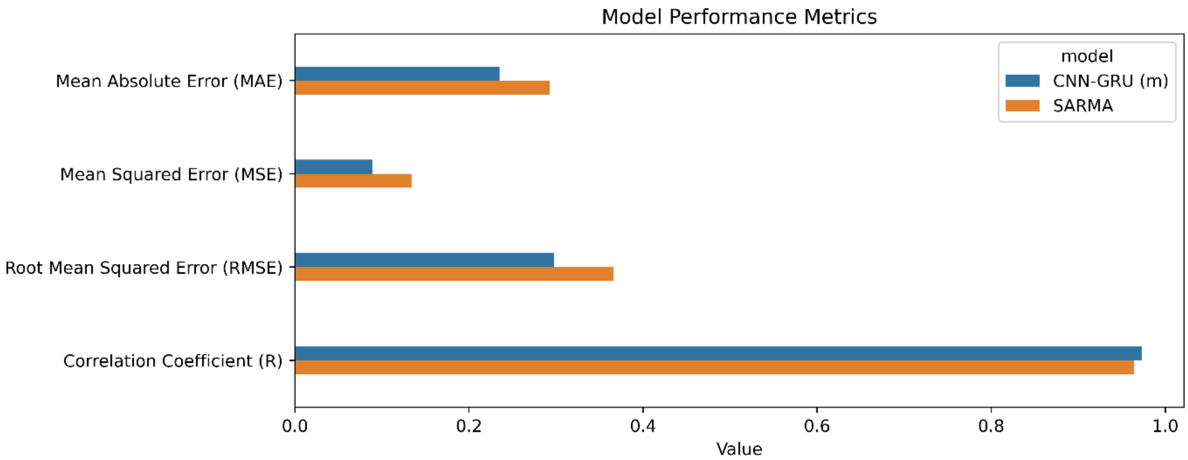

Figure 8. *Bar graph evaluation comparison of the best deep learning and statistical model.*

A visual comparison evaluation for both the CNN-GRU (m) and SARMA models is shown in Figure 8, with the former having superior performance. Figure 9 displays the predictions of both models against the test data with a 24-month horizon and indicates that the CNN-GRU (m) model achieved better alignment.

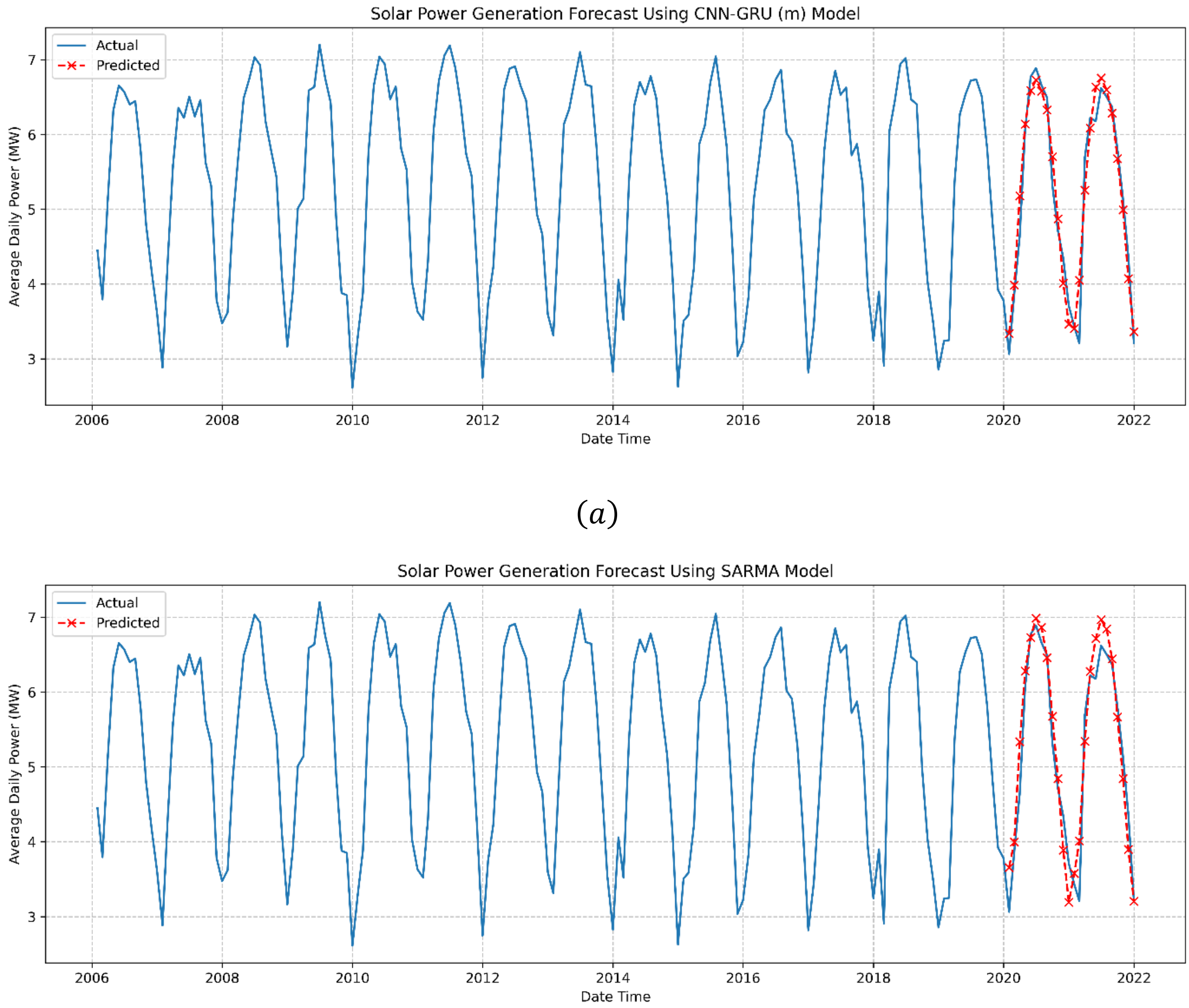

(a)

(b)

Figure 9. *Forecasting PV solar power for the next 24 months.* (a) *CNN-GRU multivariate* (b) *SARMA (D=0)*

5.0 DISCUSSION

Deriving a dataset of solar PV power values spanning from 2007 to 2021 through feature engineering using a Support Vector Regression (SVR) model, based on a single-year solar PV power generation and meteorological data, carries significant global implications. This approach offers the capability to analyse solar PV power generation across any geographical location worldwide, presenting a pathway toward addressing climate change. The incorporation of model-based features has led to the creation of abundant data for long-term forecasts, setting it apart from existing literature that predominantly relies on short time stamps with limited or negligible capacity to predict months or years in advance. According to Ieuan L.L. Griffiths (2013), Africa is commonly referred to as the "Sun continent" due to its abundant sunlight. However, several African countries lack access to electricity. By applying this model-based method with meteorological data from various African locations, governments, and business owners can strategically plan ways to provide sustainable electricity to the entire continent, thus reducing the global carbon footprint.

In time series analysis, the accuracy of a model can be considered the most important factor to consider in prediction (Fouzi Harrou & Sun, 2020). To effectively compare the prediction performance of our models with that of the existing literature, it is preferable to assess using the correlation coefficient (R) rather than the loss metrics. Loss metrics are a valuable way for model evaluation but can be influenced by factors like the capacity of the PV power generation plant and the differences in data sets.

This study uncovers the positive impact of augmenting deep learning models through the integration of convolution layers and meteorological features, leading to enhanced outcomes. Similarly, the incorporation of seasonality into our statistical models contributed to their performance improvement. In predicting 24 timesteps ahead, the CNN-GRU (m) stood out as the most robust performer among the deep learning models, achieving an impressive R value of 0.973. On the statistical front, the SARMA model performed best, securing a notable R value of 0.964. Both models were able to surpass the achievements of prior related studies, as earlier indicated, where deep learning models maintained top position.

Apart from Wang et al. (2019), whose predictions also spanned a horizon of 24 timesteps, other related research employed fewer timesteps, all having R value below 0.9. This remarkable performance can be attributed to several factors, including:

- Incorporation of convolutional and meteorological features into the deep learning model.
- Implementation of a learning rate scheduler to determine the optimal learning rate value for the deep learning model.
- Application of logarithmic transformations to enhance scaling and stationarity for both deep learning and statistical models.
- Utilization of AIC and BIC functions to achieve optimal parameters for our statistical model.
- Careful selection of window and batch sizes for the deep learning model.

Considering the computational time of prediction of our models, the statistical model tends to be more than 20 times faster than the deep learning models. This shows that the statistical models remain relevant in time series prediction, especially in short term forecasting where speed of prediction is highly considered. In the case of long-term forecasting, as demonstrated in this research, speed is of less relevance, which makes the deep learning models more suitable due to their superior prediction accuracy.

6.0 CONCLUSION

This study highlights the importance of sustainable energy sources, particularly PV solar systems, in addressing the urgent global challenge of climate change. By analysing the performance of the deep learning and statistical time series models for PV solar power generation, the deep learning method tends to exhibit more profound accuracy but requires more computational time compared to the latter. This trade-off makes the deep learning approach well-suited for long term forecasting, providing better opportunities for sustainable energy planning and climate mitigation strategies in reducing greenhouse gas emissions. The statistical model, which takes significantly less computational time, remains relevant for rapid short-term predictions where both accuracy and speed are important. The integration of convolution and meteorological features helped improve the performance of the deep-learning models. Embracing these advanced methodologies enhances our understanding and capability to harness solar power efficiently, thereby contributing to a more sustainable future.

REFERENCE

Amidi, A. & Amidi, S. (2021) *CS 230 - Recurrent Neural Networks Cheatsheet Stanford.edu*. Available online: https://stanford.edu/~shervine/teaching/cs-230/cheatsheet-recurrent-neural-networks#architecture.

Bamisile, O., Oluwasanmi, A., Obiora, S., Osei-Mensah, E., Asoronye, G. & Huang, Q. (2020) Application of deep learning for solar irradiance and solar photovoltaic multi-parameter forecast. *Energy Sources, Part A: Recovery, Utilization, and Environmental Effects*, 1–21. Available online: https://doi.org/10.1080/15567036.2020.1801903.

Brownlee, J. (2018) *Deep Learning for Time Series Forecasting*. Machine Learning Mastery.

Das, U.K., Tey, K.S., Seyedmahmoudian, M., Mekhilef, S., Idris, M.Y.I., Van Deventer, W., Horan, B. & Stojcevski, A. (2018) Forecasting of photovoltaic power generation and model optimization: A review. *Renewable and Sustainable Energy Reviews*, 81, 912–928. Available online: https://doi.org/10.1016/j.rser.2017.08.017.

Fouzi Harrou & Sun, Y. (2020) *Advanced Statistical Modeling, Forecasting, and Fault Detection in Renewable Energy Systems*. BoD – Books on Demand.

Hariharan, K. (2020) *Time Series Forecasting — ARIMA vs Prophet Medium*. Available online: https://medium.com/analytics-vidhya/time-series-forecasting-arima-vs-prophet-5015928e402a.

Huang, C., Chen, S., Yang, S. & Kuo, C. (2015) One-day-ahead hourly forecasting for photovoltaic power generation using an intelligent method with weather-based forecasting models. *IET Generation, Transmission & Distribution*, 9(14), 1874–1882. Available online: https://doi.org/10.1049/iet-gtd.2015.0175.

IEA (2020) *Renewables 2020 – Analysis IEA*. Available online: https://www.iea.org/reports/renewables-2020.

Ieuan L.l. Griffiths (2013) *The Atlas of African Affairs*. Routledge.

Jones, L.E. (2014) *Renewable energy integration: practical management of variability, uncertainty and flexibility in power grids*. London: Academic Press.

Moroney, L. (2019) *Sequences, Time Series and Prediction Coursera*. Available online: https://www.coursera.org/learn/tensorflow-sequences-time-series-and-prediction [Accessed 14/August/2023].

National Renewable Energy Laboratory (2019) *Solar Power Data for Integration Studies | Grid Modernization | NREL Nrel.gov*. Available online: https://www.nrel.gov/grid/solar-power-data.html.

National Solar Radiation Database (2019) *Home - NSRDB Nrel.gov*. Available online: https://nsrdb.nrel.gov/.

Ng, A., Mourri, Y.B. & Katanforoosh, K.K. (2017) *Convolutional Neural Networks Coursera*. Available online: https://www.coursera.org/learn/convolutional-neural-networks.

Pan, H. & Zhou, H. (2020) *Study on convolutional neural network and its application in data mining and sales forecasting for E-commerce Electronic Commerce Research*. Available online: https://www.semanticscholar.org/paper/Study-on-convolutional-neural-network-and-its-in-Pan-Zhou/56cb65874714ce9b68db8a8c4e906d447f82f29d [Accessed 23/April/2023].

Rajbhoj, A. (2019) *ARIMA simplified. Medium*. Available online: https://towardsdatascience.com/arima-simplified-b63315f27cbc.

Sharadga, H., Hajimirza, S. & Balog, R.S. (2019) Time series forecasting of solar power generation for large-scale photovoltaic plants. *Renewable Energy* [Preprint]. Available online: https://doi.org/10.1016/j.renene.2019.12.131.

Shweta (2021) *Introduction to Time Series Forecasting — Part 2 (ARIMA Models) Medium*. Available online: https://towardsdatascience.com/introduction-to-time-series-forecasting-part-2-arima-models-9f47bf0f476b.

Wang, K., Li, K., Zhou, L., Hu, Y., Cheng, Z., Liu, J. & Chen, C. (2019) Multiple convolutional neural networks for multivariate time series prediction. *Neurocomputing*, 360, 107–119. Available online: https://doi.org/10.1016/j.neucom.2019.05.023.